Hunting for the gravitational-wave background: implications for astrophysics, high energy physics, and the early Universe

Mairi Sakellariadou

KING'S College LONDON

LIGO

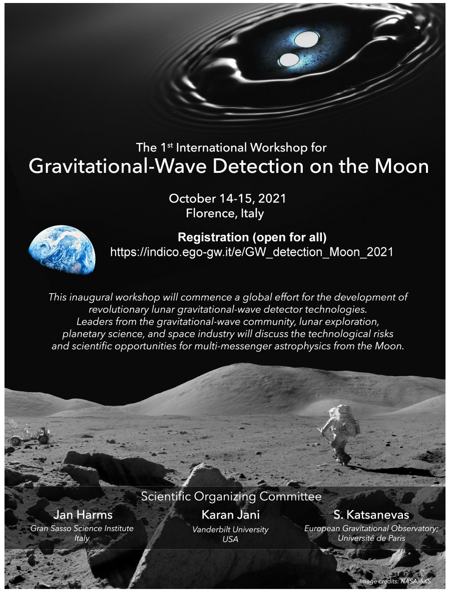

Gravitational-Wave Background (GWB)

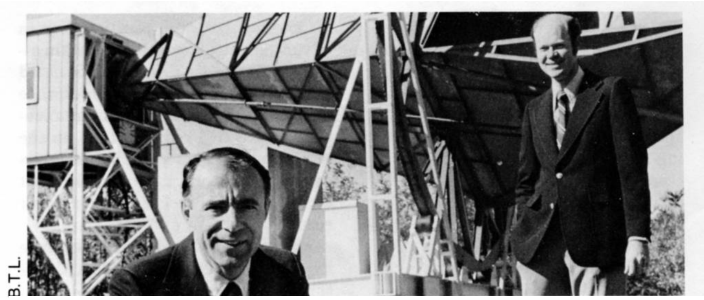

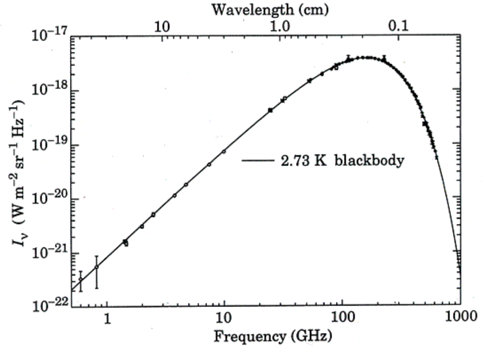

Penzias and Wilson (1965) discovered that the Universe is permeated by the CMB electromagnetic radiation

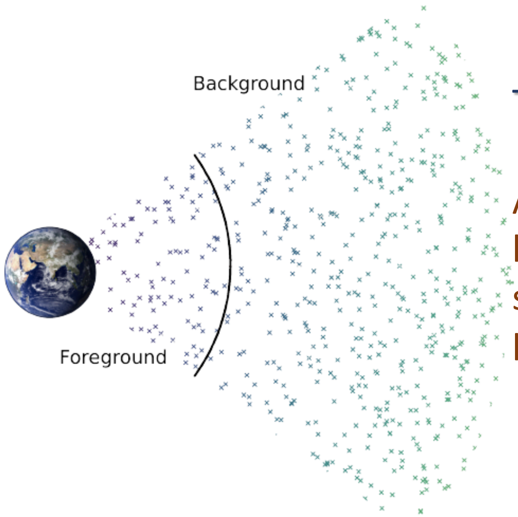

Credit: Alex Jenkins

The Universe is permeated by a stochastic GWB generated in the early Universe

A **background of GWs** can also emerge from the incoherent superposition of a large number of astrophysical sources, too weak to be detected separately, and such that the number of sources that contribute to each frequency bin is much larger than one

$$\boxed{\Omega_{\rm GW}(f) = \frac{f}{\rho_c}\frac{{\rm d}\rho_{\rm GW}}{{\rm d}f}}$$

$$\rho_{\rm GW} \sim \dot{h}^2$$

How de we detect a GWB ?

A detection of the GWB from unresolved compact binary coalescences could be made by Advanced LIGO and Advanced Virgo at their design sensitivities

It would appear as noise in a single GW detector

$$\tilde{s}_i(f) = \tilde{h}_i(f) + \tilde{n}_i(f)$$

But *noise* >> *strain*

To detect a GWB take the correlation between two detector outputs:

$$\boxed{\begin{aligned}\langle \tilde{s}_i^*(f)\tilde{s}_j(f')\rangle &= \langle \tilde{h}_i^*(f)\tilde{h}_j(f')\rangle + \langle \tilde{h}_i^*(f)\tilde{n}_j(f')\rangle \\ &\quad + \langle \tilde{n}_i^*(f)\tilde{h}_j(f')\rangle + \langle \tilde{n}_i^*(f)\tilde{n}_j(f')\rangle\end{aligned}}$$

SNR grows (slowly) over time:

$$\boxed{\langle s_1 s_2\rangle \sim \mathrm{Var}[s_1 s_2] \sim T_{\mathrm{obs}} \Rightarrow \mathrm{SNR} = \frac{\langle s_1 s_2\rangle}{\sqrt{\mathrm{Var}[s_1 s_2]}} \sim \sqrt{T_{\mathrm{obs}}}}$$

How de we detect a GWB ?

Assuming the GWB to be isotropic, Gaussian, stationary and unpolarised:

$$\langle \tilde{s}_i^*(f)\tilde{s}_j(f')\rangle = \langle \tilde{h}_i^*(f)\tilde{h}_j(f')\rangle + \langle \tilde{h}_i^*(f)\tilde{n}_j(f')\rangle + \langle \tilde{n}_i^*(f)\tilde{h}_j(f')\rangle + \langle \tilde{n}_i^*(f)\tilde{n}_j(f')\rangle$$

$\Gamma_{ij}(f)$

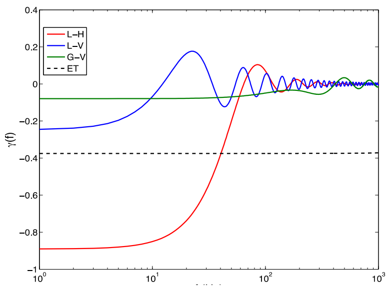

$$\boxed{\hat{C}_{ij}(f;t) = \frac{2}{T}\frac{\mathrm{Re}[\tilde{s}_i^*(f;t)\tilde{s}_j(f;t)]}{\Gamma_{ij}(f)S_0(f)}}$$

$$\boxed{S_0(f) = 3H_0^2/(10\pi^2 f^3)}$$

$$\boxed{\langle \tilde{h}_i^*(f)\tilde{h}_j(f')\rangle = \frac{1}{2}\delta_T(f-f')\Gamma_{ij}(f)S_{\mathrm{gw}}(f)}$$

Single power spectral density (PSD)

$$\boxed{S_{\mathrm{gw}}(f) = \frac{3H_0^2}{10\pi^2}\frac{\Omega_{\mathrm{gw}}(f)}{f^3}}$$

Assuming the GWB to be isotropic, Gaussian, stationary and unpolarised:

$$\langle \tilde{s}_i^*(f)\tilde{s}_j(f')\rangle = \langle \tilde{h}_i^*(f)\tilde{h}_j(f')\rangle + \cancel{\langle \tilde{h}_i^*(f)\tilde{n}_j(f')\rangle}$$
$$+\cancel{\langle \tilde{n}_i^*(f)\tilde{h}_j(f')\rangle} + \cancel{\langle \tilde{n}_i^*(f)\tilde{n}_j(f')\rangle}$$

$\Gamma_{ij}(f)$

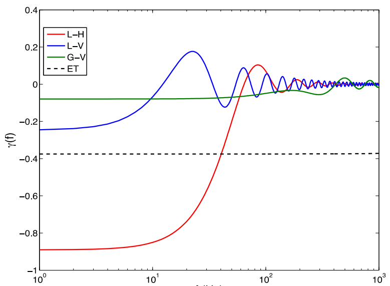

$$\boxed{\hat{C}_{ij}(f;t) = \frac{2}{T}\frac{\mathrm{Re}[\tilde{s}_i^*(f;t)\tilde{s}_j(f;t)]}{\Gamma_{ij}(f)S_0(f)}}$$

$$\boxed{S_0(f) = 3H_0^2/(10\pi^2 f^3)}$$

$$\boxed{\langle \tilde{h}_i^*(f)\tilde{h}_j(f')\rangle = \frac{1}{2}\delta_T(f-f')\Gamma_{ij}(f)S_{\rm gw}(f)}$$

Single power spectral density (PSD)

$$\boxed{S_{\rm gw}(f) = \frac{3H_0^2}{10\pi^2}\frac{\Omega_{\rm gw}(f)}{f^3}}$$

Assuming the GW signal and the intrinsic noise are uncorrelated $\langle \tilde{h}_i^*(f)\tilde{n}_j(f')\rangle = 0$ and that the noise in each frequency bin is independent

$$\langle \hat{C}_{ij}(f;t)\rangle = \Omega_{\rm gw}(f) + 2\,\mathrm{Re}\left[\frac{\langle \tilde{n}_i^*(f;t)\tilde{n}_j(f;t)\rangle}{T\Gamma_{ij}(f)S_0(f)}\right]$$

In the absence of correlated noise: $\langle \tilde{n}_i^*(f)\tilde{n}_j(f)\rangle = 0,$

$\Longrightarrow$ $\langle \hat{C}_{ij}(f)\rangle$ is an estimator for $\Omega_{\rm gw}(f)$

How de we detect a GWB ?

Assuming the GWB to be isotropic, Gaussian, stationary and unpolarised:

$$\langle \tilde{s}_i^*(f)\tilde{s}_j(f')\rangle = \langle \tilde{h}_i^*(f)\tilde{h}_j(f')\rangle + \cancel{\langle \tilde{h}_i^*(f)\tilde{n}_j(f')\rangle} + \cancel{\langle \tilde{n}_i^*(f)\tilde{h}_j(f')\rangle} + \langle \tilde{n}_i^*(f)\tilde{n}_j(f')\rangle$$

$\Gamma_{ij}(f)$

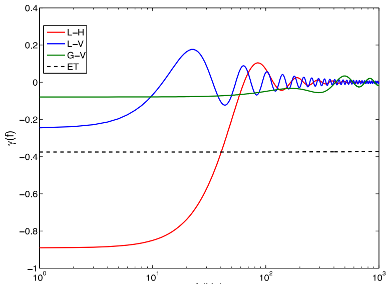

$$\boxed{\hat{C}_{ij}(f;t) = \frac{2}{T}\frac{\mathrm{Re}[\tilde{s}_i^*(f;t)\tilde{s}_j(f;t)]}{\Gamma_{ij}(f)S_0(f)}}$$

$$\boxed{S_0(f) = 3H_0^2/(10\pi^2 f^3)}$$

$$\boxed{\langle \tilde{h}_i^*(f)\tilde{h}_j(f')\rangle = \frac{1}{2}\delta_T(f-f')\Gamma_{ij}(f)S_{\rm gw}(f)}$$

Single power spectral density (PSD)

$$\boxed{S_{\rm gw}(f) = \frac{3H_0^2}{10\pi^2}\frac{\Omega_{\rm gw}(f)}{f^3}}$$

Assuming the GW signal and the intrinsic noise are uncorrelated $\langle \tilde{h}_i^*(f)\tilde{n}_j(f')\rangle = 0$ and that the noise in each frequency bin is independent

$$\langle \hat{C}_{ij}(f;t)\rangle = \Omega_{\rm gw}(f) + 2\,\mathrm{Re}\left[\frac{\langle \tilde{n}_i^*(f;t)\tilde{n}_j(f;t)\rangle}{T\Gamma_{ij}(f)S_0(f)}\right]$$

In the absence of correlated noise: $\langle \tilde{n}_i^*(f)\tilde{n}_j(f)\rangle = 0,$

$\Longrightarrow$ $\langle \hat{C}_{ij}(f)\rangle$ is an estimator for $\Omega_{\rm gw}(f)$

what if:

$$\boxed{\langle \tilde{n}_i^*(f)\tilde{n}_j(f)\rangle \neq 0}$$

How are we sure that there is a real GWB detection?

Schumann Resonances

- Resonances in the global electromagnetic field of Earth
- **Correlated** magnetic noise contamination

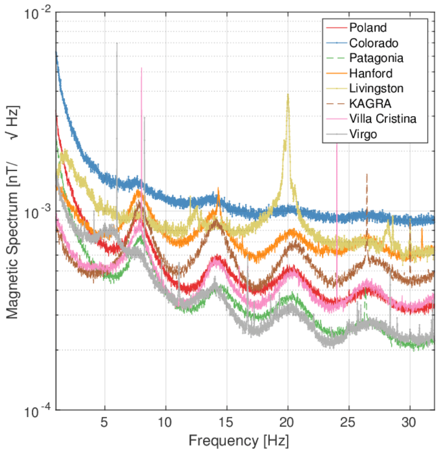

Median power spectral density of magnetometers. [1802.00885]

$$\langle \hat{C}_{ij}(f) \rangle = \Omega_{\rm gw}(f) + \Omega_{{\rm M},ij}(f),$$

magnetic contribution

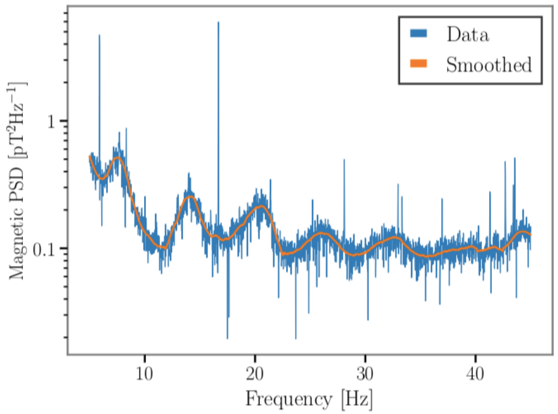

Power spectral density of magnetometer data near aVIRGO, showing 5 harmonics of Schumann resonances

Meyers, Martinovic, Christensen, Sakellariadou, PRD102 (2020) 10, 102005

Joint magnetic + GWB fit

- A ***novel approach***, complementary to the magnetic noise budget
- We model the background from the local magnetic field $$\langle \tilde{m}_i^*(f)\tilde{m}_j(f')\rangle = \frac{1}{2}\delta_T(f-f')\gamma_{ij}^M(f)M(f),$$
  correlated magnetic power spectral density
- We model its coupling to the strain channel of the detectors, via the transfer function

$$T(f) = \kappa\left(\frac{f}{10\ \mathrm{Hz}}\right)^{-\beta} \times 10^{-23}\ \mathrm{strain/pT},$$

Correlated noise in the GW detectors induced by the magnetic fields

$$\tilde{n}(f) = T(f)\tilde{m}(f)$$

Magnetic contribution:

$$\boxed{\Omega_{\mathrm{M},ij}(f) = \kappa_i\kappa_j\left(\frac{f}{10\ \mathrm{Hz}}\right)^{-\beta_i-\beta_j}\hat{M}_{ij}(f)\times 10^{-22}}$$

Meyers, Martinovic, Christensen, Sakellariadou, PRD102 (2020) 10, 102005

Using the detector network

Advantages of a detector network in GWB searches

- Improves **high-frequency sensitivity**
- Distinguish between different **polarisations**

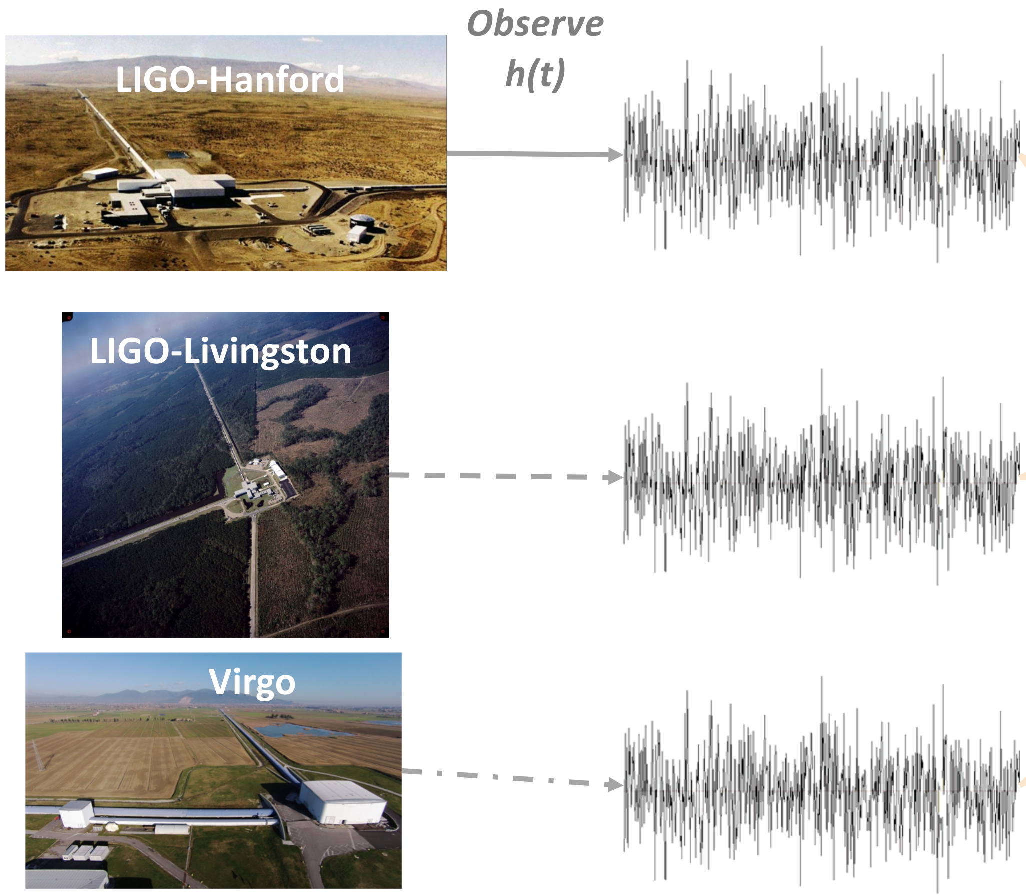

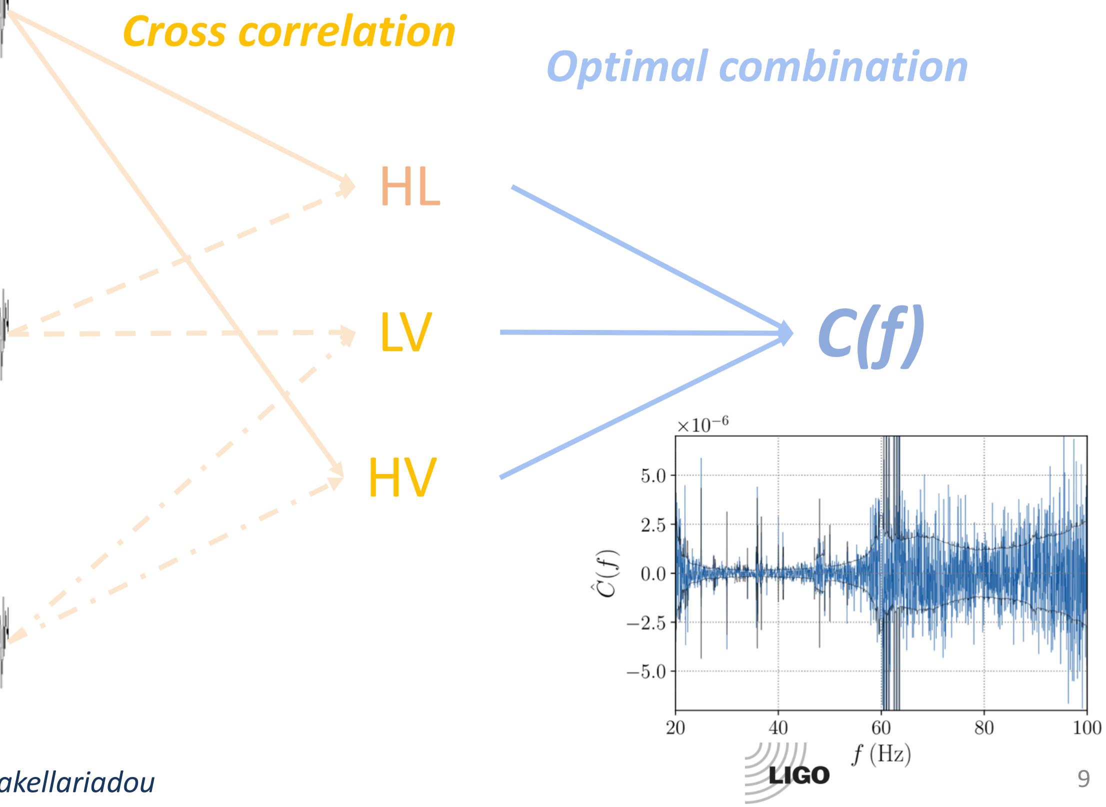

O3 LVK Collaboration: GWB searches

Cross-correlation spectra and parameter estimation formalism

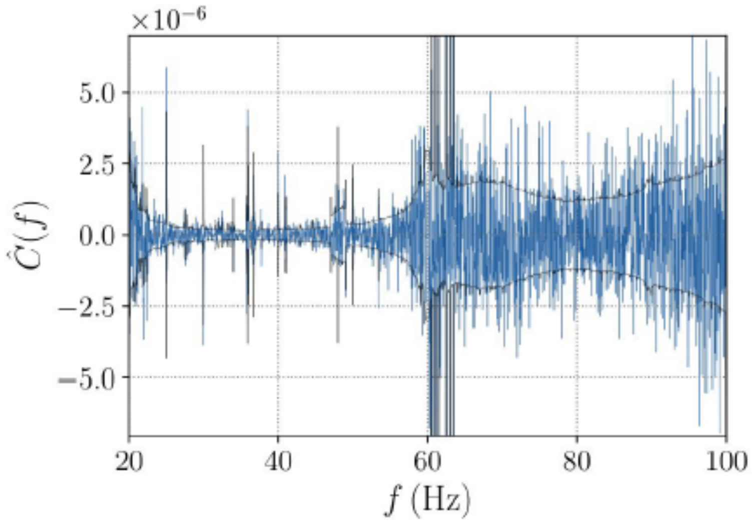

We fit models to O3 data using a hybrid frequentist-Bayesian approach:

multi-baseline Gaussian likelihood

$$p(\hat{C}_k^{IJ}|\boldsymbol{\Theta}) \propto \exp\left[-\frac{1}{2}\sum_{IJ}\sum_{k}\left(\frac{\hat{C}_k^{IJ} - \Omega_{\rm M}(f_k|\boldsymbol{\Theta})}{\sigma_{IJ}(f_k)}\right)^2\right]$$

- H, L and V baselines combined for the first time
- O3 data consistent with uncorrelated, Gaussian noise

- Gaussian noise preferred over correlated magnetic noise

$$\log_{10}\mathcal{B}_{\rm N}^{\rm MAG} = -0.03$$

- Gaussian noise preferred over correlated magnetic noise + power law GWB

$$\log_{10}\mathcal{B}_{\rm N}^{\rm MAG+PL} = -0.3$$

LVK Collaboration, PRD 104 (2021), 2, 022004

Upper limits on power-law backgrounds:

2 parameters in the power-law model:

$$\Omega_{\rm PL}(f) = \Omega_{\rm ref}\left(\frac{f}{f_{\rm ref}}\right)^{\alpha}$$

We place upper limits on $\Omega_{\rm ref}$ for different priors:

	Log-uniform prior		
α	O3	O2	Improvement
0	5.8×10^{-9}	3.5×10^{-8}	6.0
2/3	3.4×10^{-9}	3.0×10^{-8}	8.8

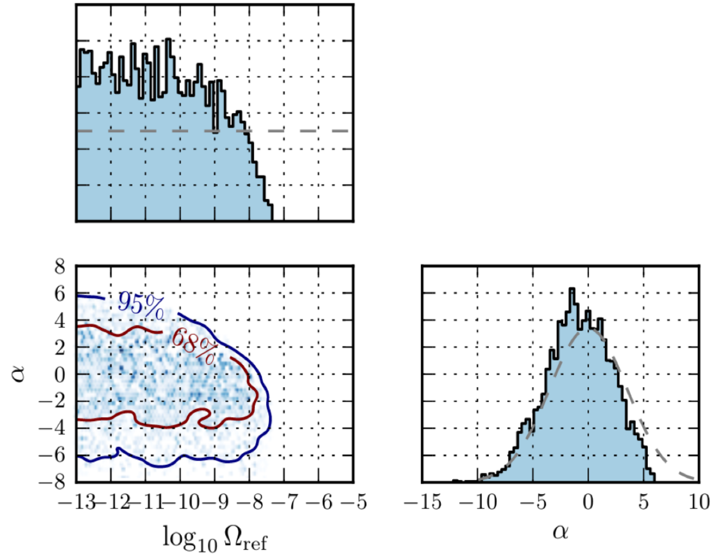

LVK Collaboration, PRD 104 (2021), 2, 022004

Search for non-GR polarisations: information about theories of gravity

Alternative theories of gravity: scalar (S), vector (V), tensor (T) polarisations

$$\boxed{\Omega_{\mathrm{SVT-PL}}(f) = \sum_{\mathrm{p}} \beta_{IJ}^{(\mathrm{p})}(f)\Omega_{\mathrm{ref}}^{(\mathrm{p})}\left(\frac{f}{f_{\mathrm{ref}}}\right)^{\alpha_{\mathrm{p}}}} \quad \mathrm{p} = \{\mathrm{T}, \mathrm{V}, \mathrm{S}\};$$

$$\beta_{IJ}^{(\mathrm{p})}(f) = \gamma_{IJ}^{(\mathrm{p})}(f)/\gamma_{IJ}(f)$$

Current generation (number, orientation) of detectors cannot determine polarisation of transient GW signals

even if the LIGO detectors were more favorably-oriented -- now nearly co-oriented -- a network of at least 6 detectors in required to uniquely determine the polarization (2 vector, 2 scalar, 2 tensor) modes

Bayesian method to detect and characterise the polarisation of the GWB

Callister, et al (Sakellariadou), PRX 7 (2017) 041058

Constrains on the strain power in each polarisation

(log-uniform prior for Ω_{ref} *and a Gaussian prior on the spectral index)*

Polarization	O3	O2	Improvement
Tensor	6.4×10^{-9}	3.2×10^{-8}	5.0
Vector	7.9×10^{-9}	2.9×10^{-8}	3.7
Scalar	2.1×10^{-8}	6.1×10^{-8}	2.9

There is no evidence of non-GR polarisations

The non-detection of scalar and vector polarised GW is consistent with predictions of GR

LVK Collaboration, PRD 104 (2021), 2, 022004

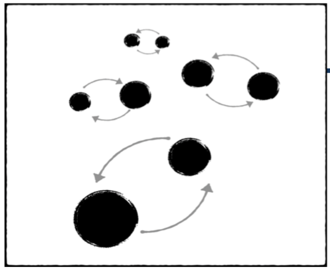

GWB from compact binary coalescence (CBC)

$$\Omega_{\rm GW}(\nu) = \Omega_{\rm ref}\left(\frac{\nu}{\nu_{\rm ref}}\right)^{\alpha}$$

α=2/3

$$\nu_{\rm ref} = 25\text{Hz}$$

$$\frac{dE_{\rm GW}}{d\nu} = \frac{(G\pi)^{2/3}}{3}\frac{m_1 m_2}{(m_1+m_2)^{1/3}}\nu^{-1/3}$$

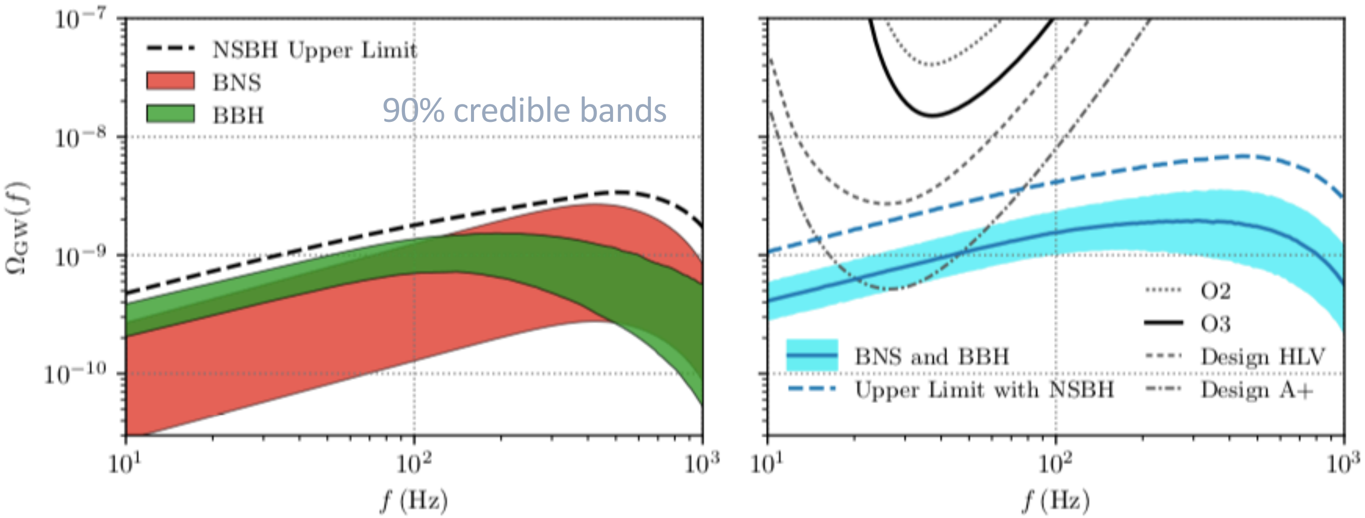

$$\Omega_{\rm GW} \ll \Omega_{\rm CMB} \approx 10^{-5}$$

$$\boxed{\Omega_{\rm GW}(f) \leq 3.4\times 10^{-9} \quad \text{at } 25 \text{ Hz}}$$

So, detection is indeed hard!

LVK Collaboration, PRD 104 (2021), 2, 022004

GWB from CBC: info about Compact Binaries

$$\Omega_{\mathrm{GW}}(\nu,\theta) = \frac{\nu}{\rho_c H_0} \int_0^{z_{\max}} \mathrm{d}z \, \frac{R_{\mathrm{m}}(z;\theta) \frac{\mathrm{d}E_{\mathrm{GW}}(\nu_{\mathrm{s}};\theta)}{\mathrm{d}\nu_{\mathrm{s}}}}{(1+z)E(\Omega_{\mathrm{M}},\Omega_{\Lambda},z)}$$

$$E(\Omega_{\mathrm{M}},\Omega_{\Lambda},z) = \sqrt{\Omega_{\mathrm{M}}(1+z)^3 + \Omega_{\Lambda}}$$

$$\nu_{\mathrm{s}} = (1+z)\nu$$

Most important quantities describing each BBH are the **masses** and **spins** of each component BH

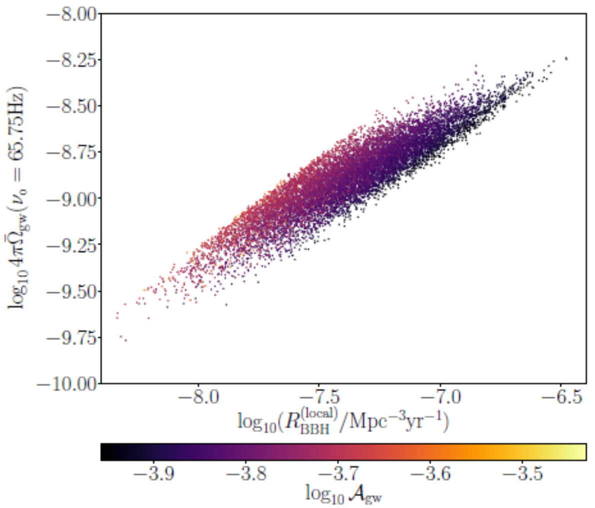

Truncated power-law BH mass distribution:

$$p(m_1,m_2) \propto \begin{cases} \frac{m_1^{-\alpha_m}}{m_1 - m_{\min}}, & m_{\min} \le m_2 \le m_1 \le m_{\max} \\ & m_1 + m_2 \le M_{\max} \\ 0, & \text{otherwise} \end{cases}$$

$$m_{\min} = 5M_{\odot}$$

$$M_{\max} = 200M_{\odot}$$

Beta distribution for the BH spins:

$$p(\chi_i) \propto \chi_i^{\alpha_\chi - 1}(1-\chi_i)^{\beta_\chi - 1}$$

α_m, $m_{\max}$, α_χ, β_χ — *infrerred from observed BBHs*

Wysocki, Lange, O'Shaughnessy (2018)

The **total energy density varies over nearly two orders of magnitude**

a new probe of population of compact objects

Jenkins, O'Shaughnessy, Sakellariadou, Wysocki, PRL 122, 111101 (2019)

SGWB from cosmic strings: info beyond Standard Model

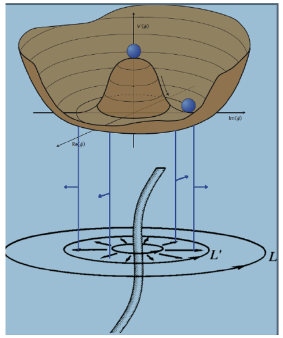

1dim topological defects formed in the early universe as a result of a PT followed by SSB, characterised by a vacuum manifold with non-contractible closed curves

$$G \to \cdots \to G_{\rm SM} \qquad \pi_1(\mathcal{M}) \neq 0$$

Kibble (1976)

Generically formed in the context of GUTs

Jeannerot, Rocher, Sakellariadou, PRD68 (2003) 103514

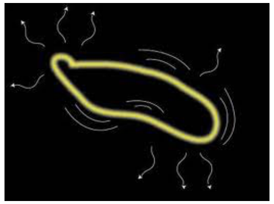

CS loops (length ℓ) oscillate periodically ($T = \ell/2$) in time emitting GWs (fundamental frequency $\omega = 4\pi/\ell$)

$$\boxed{\tau \sim \frac{\ell}{G\mu}}$$

$$G\mu \sim T^2_{\rm SSB}$$

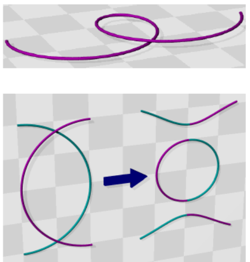

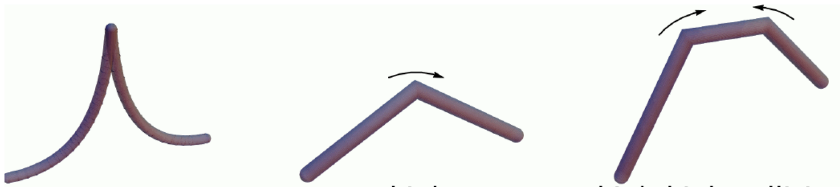

cusp	kink	kink-kink collision
$\tilde{h} \sim f^{-4/3}$	$\tilde{h} \sim f^{-5/3}$	$\tilde{h} \sim f^{-2}$
beamed	beamed	isotropic

Oscillating loops of cosmic strings generate a SGWB that is strongly non-Gaussian, and includes occasional sharp bursts due to cusps and kinks

SGWB from cosmic strings: info beyond Standard Model

$$\bar{\Omega}_{\mathrm{gw}} = \frac{2(G\mu)^2}{3\pi^2 H_0^2 \nu_o} \int_0^{t_*} \frac{\mathrm{d}t}{t^4} a^5 \int_0^{\gamma_*} \frac{\mathrm{d}\gamma}{\gamma} \bar{\mathcal{F}} \Theta\left(\gamma - \frac{2a}{\nu_o t}\right) \left[N_{\mathrm{k}}^2 + 4A N_{\mathrm{k}} \left(\frac{\nu_o \gamma t}{a}\right)^{1/3} + A^2 N_{\mathrm{c}} \left(\frac{\nu_o \gamma t}{a}\right)^{2/3} \right]$$

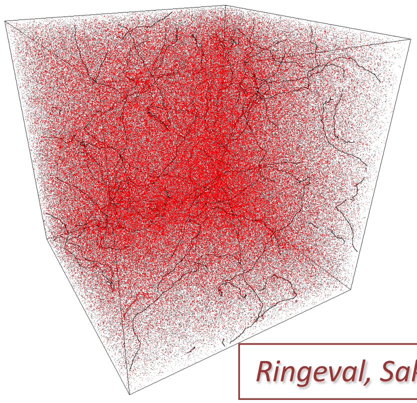

Ringeval, Sakellariadou, Bouchet (2007)

$$G\mu = \frac{\text{mass}}{\text{length}} \sim \left(\frac{\text{new physics scale}}{\text{Planck scale}}\right)^2 \ll 1$$

$$G\mu \sim T_{\mathrm{SSB}}^2$$

Model A: Blanco-Pillado, Olum, Shlaer (2014)
Model B: Lorenz, Ringeval, Sakellariadou (2010)
Model C: Auclair, Ringeval, Sakellariadou, Steer (2019)

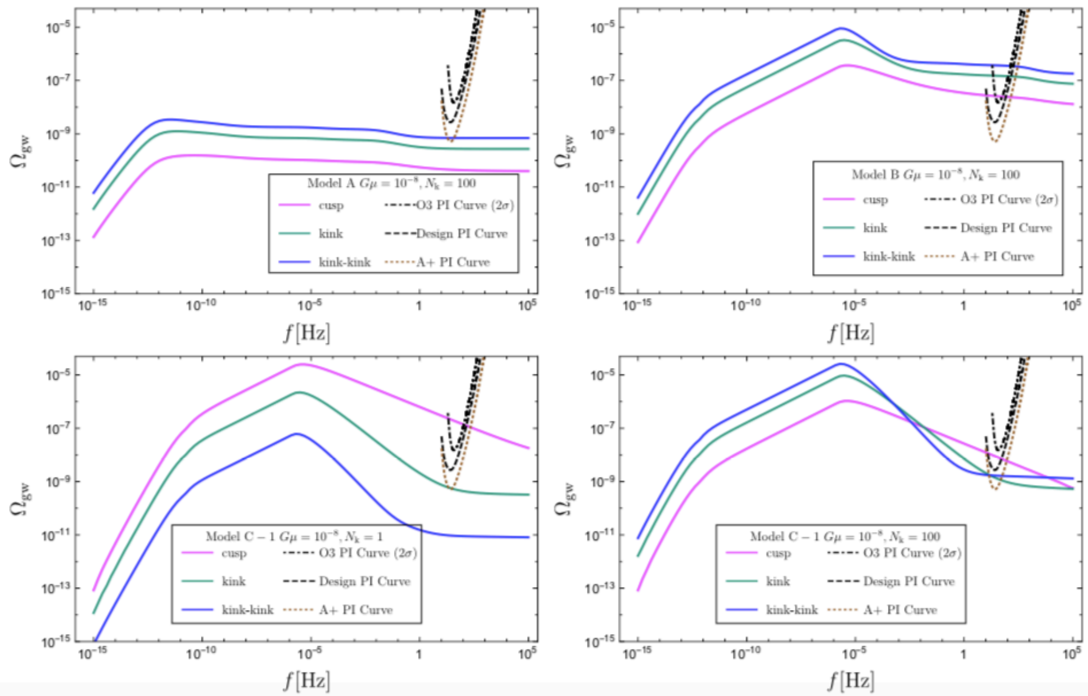

LVK Collaboration, PRL 126 (2021) 24, 241102

SGWB from cosmic strings: info Beyond the Standard Model

Excluded regions:

Model A: $G\mu \gtrsim (9.6 \times 10^{-9} - 10^{-6})$

strongest limit from PTA $G\mu \gtrsim 10^{-10}$

Model B: $G\mu \gtrsim (4.0 - 6.3) \times 10^{-15}$
strongest limit from LVK stochastic

Model C1: $G\mu \gtrsim (2.1 - 4.5) \times 10^{-15}$
strongest limit from LVK stochastic

Model C2: $G\mu \gtrsim (4.2 - 7.0) \times 10^{-15}$
strongest limit from LVK stochastic

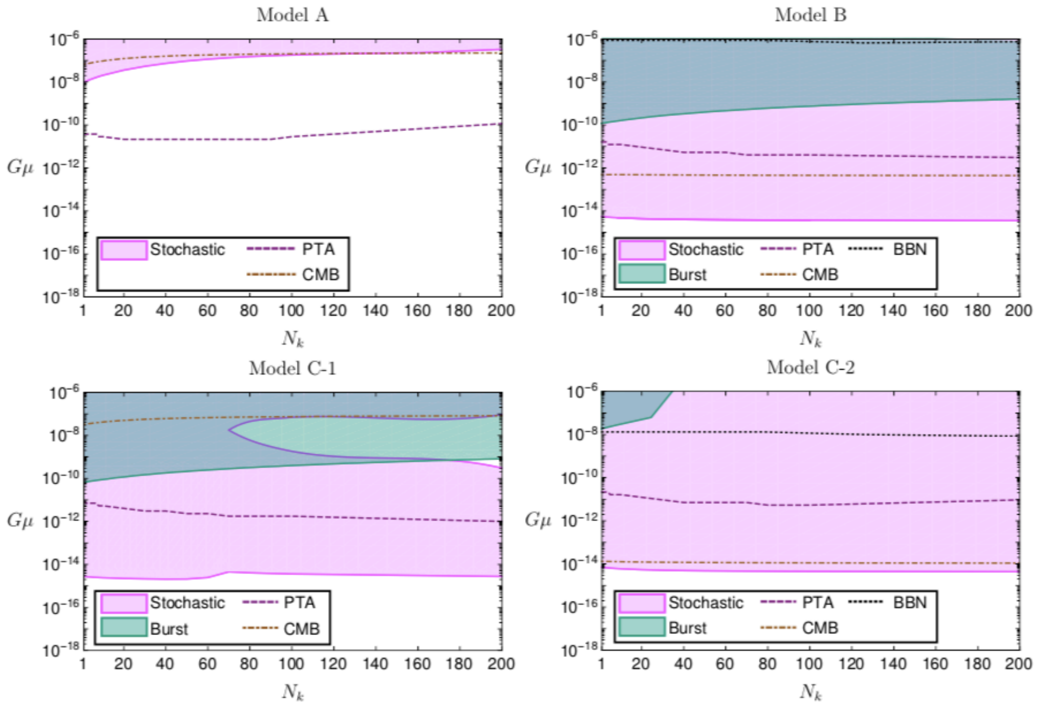

Model A: Blanco-Pillado, Olum, Shlaer (2014)
Model B: Lorenz, Ringeval, Sakellariadou (2010)
Model C: Auclair, Ringeval, Sakellariadou, Steer (2019)

LVK Collaboration, PRL 126 (2021) 24, 241102

SGWB from cosmic strings: info Beyond the Standard Model

Excluded regions:

Model A: $G\mu \gtrsim (9.6 \times 10^{-9} - 10^{-6})$

strongest limit from PTA $G\mu \gtrsim 10^{-10}$

Model B: $G\mu \gtrsim (4.0 - 6.3) \times 10^{-15}$
strongest limit from LVK stochastic

Model C1: $G\mu \gtrsim (2.1 - 4.5) \times 10^{-15}$
strongest limit from LVK stochastic

Model C2: $G\mu \gtrsim (4.2 - 7.0) \times 10^{-15}$
strongest limit from LVK stochastic

Energy scale $\approx \sqrt{\frac{G\mu}{10^{-10}}} 10^{14}\mathrm{GeV}$

Energy scale	Width	Linear density
GUT : 10^{16} GeV	2×10^{-32} m	$G\mu \approx 10^{-6}$
3×10^{10} GeV	5×10^{-27} m	$G\mu \approx 10^{-17}$
10^{8} GeV	2×10^{-24} m	$G\mu \approx 10^{-22}$
EW : 100 GeV	2×10^{-18} m	$G\mu \approx 10^{-34}$

Model A: Blanco-Pillado, Olum, Shlaer (2014)
Model B: Lorenz, Ringeval, Sakellariadou (2010)
Model C: Auclair, Ringeval, Sakellariadou, Steer (2019)

LVK Collaboration, PRL 126 (2021) 24, 241102

SGWB from cosmic strings: info Beyond the Standard Model

LISA will be able to probe cosmic strings with tensions $G\mu \gtrsim \mathcal{O}(10^{-17})$

Auclair et al (Sakellariadou), JCAP (2020)

But …

- instrumental noise

- **astrophysical background from CBCs**
- **galactic foreground from WD binaries**

A CS tension in the $G\mu \approx 10^{-16}$ to $G\mu \approx 10^{-15}$ range or bigger could be measured by LISA, with the galactic foreground affecting this limit more than the astrophysical background

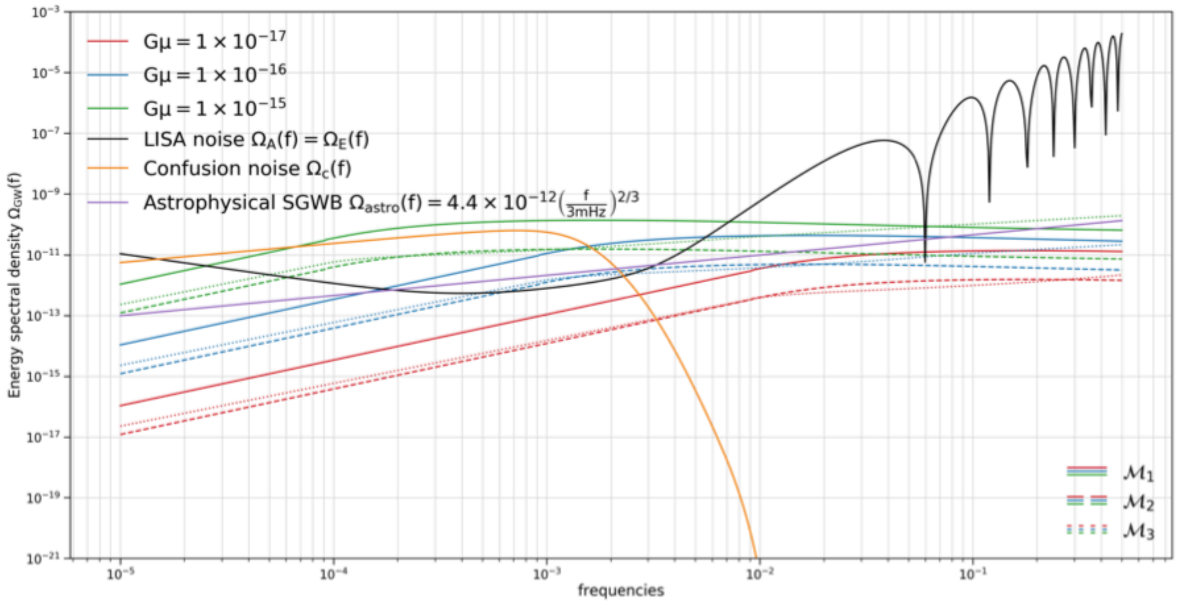

Boileau, Jenkins, Sakellariadou, Meyer, Christensen (2021)

SGWB from first order phase transition(FOPT): info Beyond the Standard Model

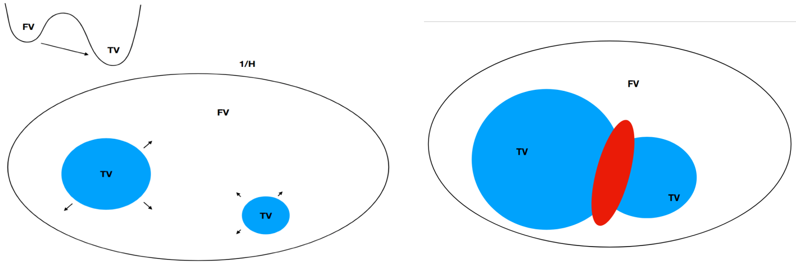

Sources of GWs:

- **Sound waves** (coupling between scalar field and thermal bath)
- **Bubble collisions**
- Magnetohydrodynamic turbulence

SGWB: broken power law with peak frequency mainly determined by temperature of FOPT

If $T_{\rm pt} \sim (10^7 - 10^9)\ {\rm GeV}$ (not accessible by LHC) : **SGWB is within aLIGO/aVIRGO**

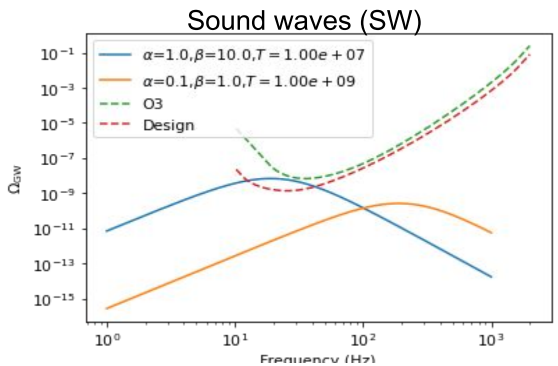

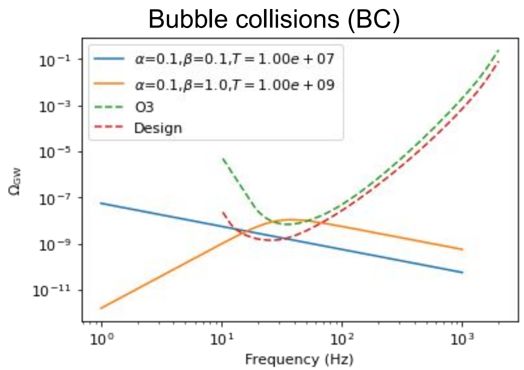

O1+O2+O3:

$$\Omega_{\rm CBC} < 6.1 \times 10^{-9}$$
$$\Omega_{\rm BPL} < 4.4 \times 10^{-9}$$

Romero, Martinovic, Callister, Guo, Martinez, Sakellariadou, Yang, Zhao, PRL 126 (2021) 15, 151301

α : strength of FOPT

β : inverse duration of FOPT

Footprints of pop III stars in the GWB

2G detector networks: pop III is practically invisible and its contribution to the global SNR is negligible

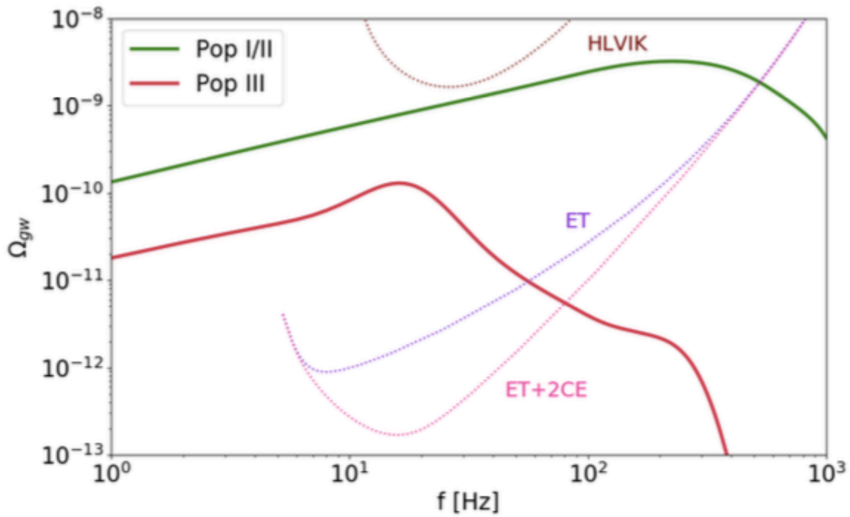

To uncover pop III stars, we need to look at residual backgrounds, i.e. to subtract individually detected merger events

Martinovic, Perigois, Regimbau, Sakellariadou, 2109.09779

Footprints of pop III stars in the GWB

2G detector networks: pop III is practically invisible and its contribution to the global SNR is negligible

3G detectors may reveal a pop III background

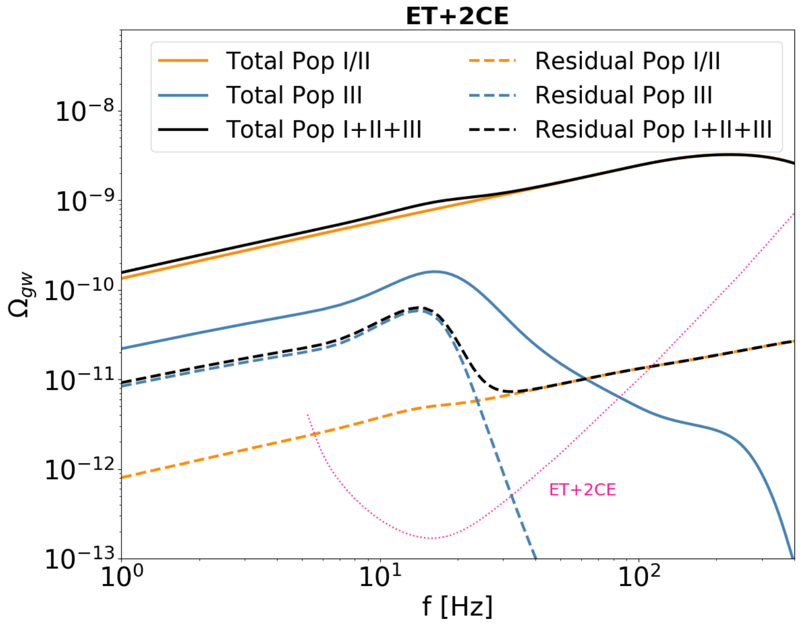

ET + 2CE: we uncover pop III after the subtraction of individually resolved merger events

- Subtraction methods are less efficient to detect the high-z and low-f pop III CBCs

- Being more difficult to resolve, binaries from pop III persist, resulting in a large contribution to the residual CBC background (dominant for f below ~ 20 Hz)

Martinovic, Perigois, Regimbau, Sakellariadou, 2109.09779

Footprints of pop III stars in the GWB

model, $\mathcal{M}$	ln $\mathcal{B}_{2/3}^{\mathcal{M}}$
power law	29 000
broken power law	46 000
smooth broken power law	47 000
triple broken power law	46 000

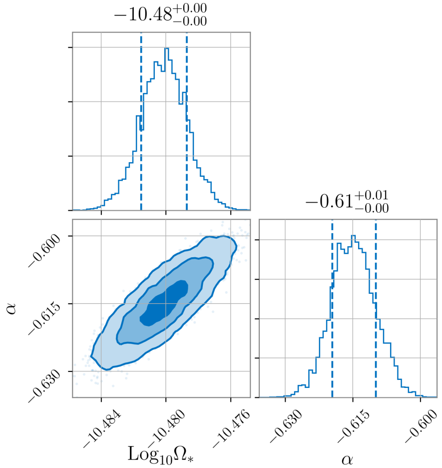

Varying-α power law fit to residual GWB spectrum of pop I+II+III from the ST simulation.
The α estimate is different from the characteristic 2/3 for the inspiral phase

These further away stars will lead to more redshifted frequencies and therefore be detected in their merger and ringdown phases

We can constrain very well the peak frequency of the spectrum with a broken power law filter

Relationship between peak frequency and redshifted total mass $M^z_{\rm tot} = (1+z)(m_1+m_2)$

Detection of pop III GWB and estimation of the peak frequency could reveal important information, such as the average redshifted total mass

Martinovic, Perigois, Regimbau, Sakellariadou, 2109.09779

SGWB from second order scalar perturbations: information about early universe

- PBH formation through large curvature perturbations during inflation

⇨ **Strong SGWB generated at 2nd order in perturbation theory from scalar perturbations**

O1+O2+O3: upper limits on the amplitude of power spectrum and on the fraction of the DM in terms of ultralight PBHs

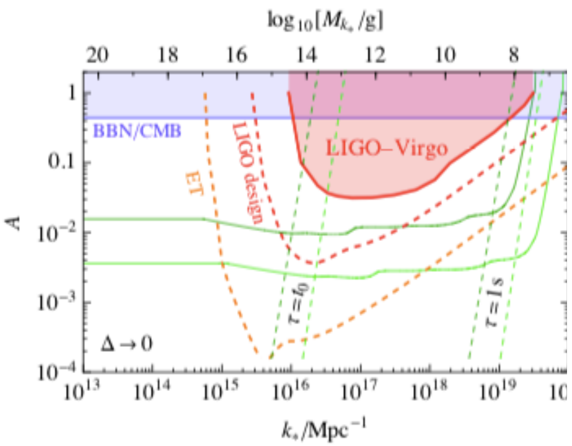

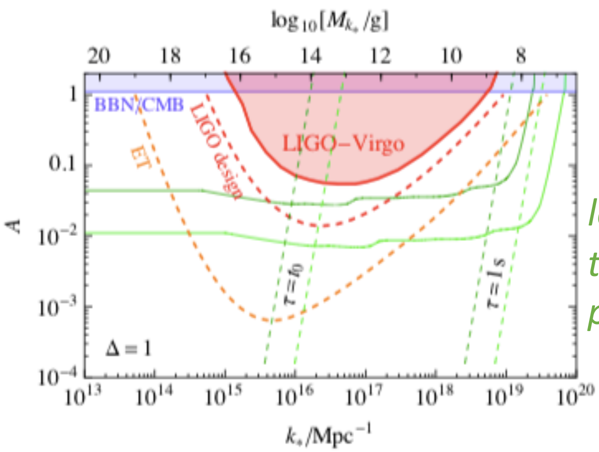

Integrated power of peak

position of peak

$$\mathcal{P}_\zeta(k) = \frac{A}{\sqrt{2\pi}\Delta}\exp\left[-\frac{\ln^2(k/k_*)}{2\Delta^2}\right]$$

width of peak

log-normal shape for the peak in curvature power spectrum

For LIGO/Virgo sensitivity: $M_{\mathrm{PBH}} \lesssim 10^{16}\,\mathrm{g}.$

No evidence for such a SGWB

95% CL upper limits on integrated power of the curvature power spectrum peak down to 0.02 at $10^{17}\,\mathrm{Mpc}^{-1}$

Romero-Rodriguez, Martinez, Pujolas, Sakellariadou, Vaskonen 2107.11660

Gravitational parity violation: info about the early universe

Observed matter-antimatter asymmetry in the radiation era requires sources of parity violation (Sakharov criteria, 1967)

- Early universe mechanisms can create parity violation → production of asymmetric amounts of right- and left-handed circularly polarised isotropic GWs
- Astrophysical GWB sources are unlikely to have circular polarisation

- Detection of parity violation can allow cosmologically sourced GWs to be distinguished from the astrophysically sourced component of the GWB
- Analysis of polarised GWB can place constraints on parity violating theories

- *Chern-Simons gravitational term* *Yagi, Yang (2018)*
- *Axion inflation* *Crowder, Namba, Mandic, Mukoyama, Peloso (2013)*
- *Turbulence in the primordial plasma: FOPT (EW or QCD) or primordial magnetic fields coupled to cosmological plasma* *Martinovic, Badger, Sakellariadou, Mandic, PRD 2021*

Gravitational parity violation: info about the early universe

$$\begin{pmatrix} \langle h_R(f,\hat{\Omega}) h_R^*(f',\hat{\Omega}') \rangle \\ \langle h_L(f,\hat{\Omega}) h_L^*(f',\hat{\Omega}') \rangle \end{pmatrix} = \frac{\delta(f-f')\delta^2(\hat{\Omega}-\hat{\Omega}')}{4\pi} \begin{pmatrix} I(f,\hat{\Omega}) + V(f,\hat{\Omega}) \\ I(f,\hat{\Omega}) - V(f,\hat{\Omega}) \end{pmatrix}$$

For V=0: the correlator of unpolarised GWB

Cross-correlator estimator

$$\Omega'_{\mathrm{GW}} = \Omega_{\mathrm{GW}} \left[1 + \Pi(f) \frac{\gamma_V^{d_1 d_2}(f)}{\gamma_I^{d_1 d_2}(f)} \right]$$

Polarisation degree $\Pi(f) = V(f)/I(f)$

- -1 : fully L polarisation
- 1 : fully R polarisation
- 0 : unpolarised isotropic SGWB

O1+O2+O3: No evidence for polarisation

There are two relevant SGWB upper limits:

- One that confirms presence of polarised GW signal
- A larger one that estimates the degree of polarisation with confidence

Even if we detect a turbulence signal, we may **not** be able to deduce its polarisation

Martinovic, Badger, Sakellariadou, Mandic , PRD 2021

Can we distinguish between astrophysical vs cosmological sources?

GW models:

- CBC background

$$\Omega_{\rm CBC}(f) = \Omega_{2/3}\left(\frac{f}{25\ \rm Hz}\right)^{2/3}$$

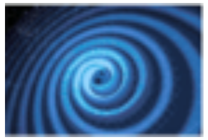

- CS background (flat)

$$\Omega_{\rm CS}(f) = \rm const.$$

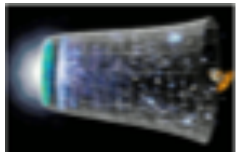

- PT background (smooth broken power law (BPL))

$$\Omega_{\rm BPL} = \Omega_{*}\left(\frac{f}{f_*}\right)^{\alpha_1}\left[1+\left(\frac{f}{f_*}\right)^{\Delta}\right]^{(\alpha_2-\alpha_1)/\Delta}$$

we fix $\alpha_1 = 3, \alpha_2 = -4, \Delta = 2$ to approximate sound waves contribution

Martinovic, Meyers, Sakellariadou, Christensen, PRD 103 (2021) 4, 043023

Can we distinguish between astrophysical vs cosmological sources?

log-likelihood for a single detector pair

$$\log p(\hat{C}_{ij}(f)|\boldsymbol{\theta}_{\rm GW}) = -\frac{1}{2}\sum_f \frac{\left[\hat{C}_{ij}(f) - \Omega_{\rm GW}(f,\boldsymbol{\theta}_{\rm GW})\right]^2}{\sigma_{ij}^2(f)} - \frac{1}{2}\sum_f \log\left[2\pi\sigma_{ij}^2(f)\right]$$

CBC Power Law: $\boldsymbol{\theta} = (\Omega_{2/3})$,
CBC + CS: $\boldsymbol{\theta} = (\Omega_{2/3}, \Omega_{\rm CS})$.
CBC + BPL: $\boldsymbol{\theta} = (\Omega_{2/3}, \Omega_*, f_*)$.

Model selection — To compare two models we use Bayes factors

Detector networks

- Hanford, Livinston, Virgo, O4 sensitivity, 1 year of run time
- Cosmic Explorers (CE) at Hanford and Livingston locations, Einstein Telescope (ET) at Virgo, 1 year of run time

- Current GW detectors are unable to separate astrophysical from cosmological sources
- Future GW detectors (CE, ET) can dig out cosmological signals, provided one can **subtract the *loud* astrophysical foreground**

Martinovic, Meyers, Sakellariadou, Christensen, PRD 103 (2021) 4, 043023

BBH will not limit observation of primordial backgrounds, but BNS population will limit sensitivity of 3G detectors to about $\Omega_{\rm GW} \sim 10^{-11}$ at 10 Hz

Sachdev, Regimbau, Sathyaprakash (2020)

Anisotropies in the GW Background: info about large-scale-structure

To a first approximation, the SGWB is assumed to be isotropic (analogous to the CMB)

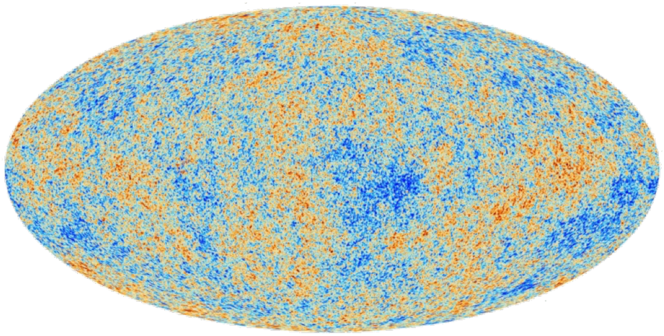

The afterglow radiation left over from the Hot Big Bang

- its temperature is extremely uniform all over the sky
- **tiny temperature fluctuations** (one part 100,000)

$$C_\ell = \int \mathrm{d}^2\hat{\boldsymbol{n}} P_\ell(\cos\theta) \left\langle \delta T_\gamma \delta T_\gamma \right\rangle_\theta$$

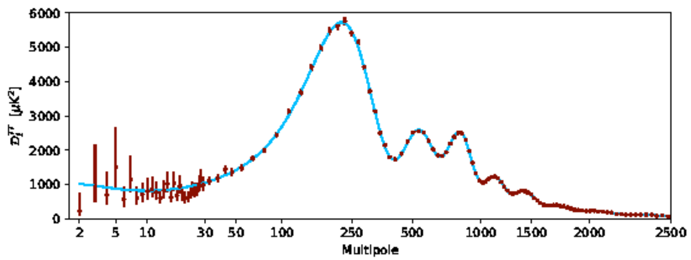

Image credit: Planck collaboration

LSS

SGWB

$$C_\ell = \int \mathrm{d}^2\hat{\boldsymbol{n}} P_\ell(\cos\theta) \left\langle \delta\Omega_{\mathrm{GW}} \delta\Omega_{\mathrm{GW}} \right\rangle_\theta$$

Anisotropies in the GW Background: info about large-scale-structure

Gravitational wave sources with an anisotropic spatial distribution lead to a GWB characterised by preferred directions, and hence anisotropies

$\alpha = 0$ $\alpha = 2/3$ $\alpha = 3$

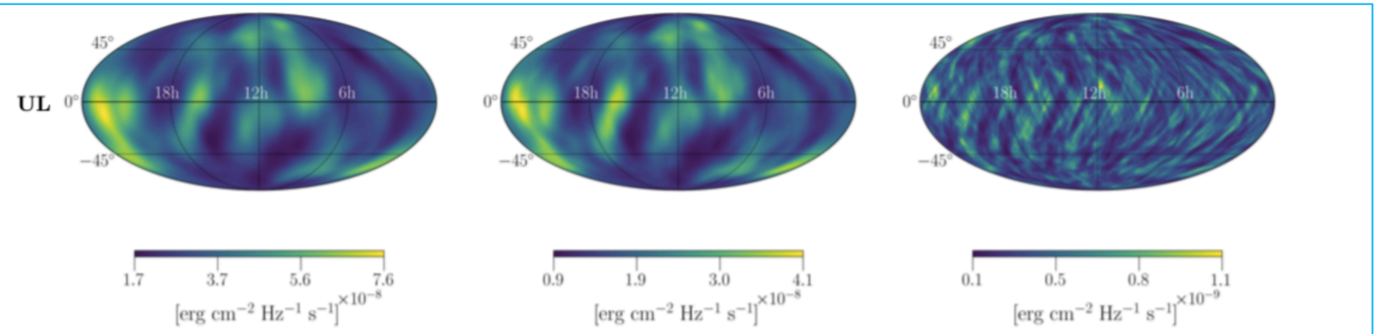

Upper limits sky maps of GWs energy flux from a search from point-like sources

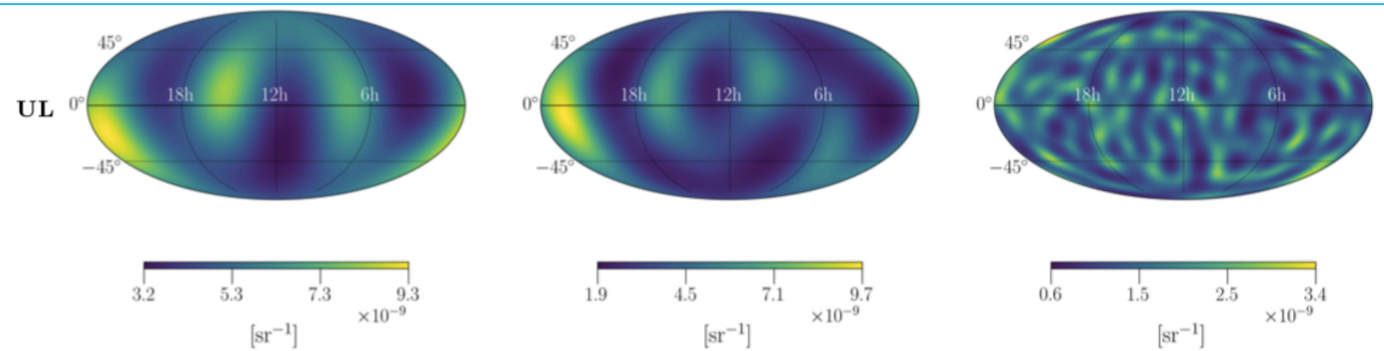

Upper limits sky maps of GWs energy flux from a search from extended sources

Anisotropies in the GW Background: info about large-scale-structure

Gravitational wave sources with an anisotropic spatial distribution lead to a GWB characterised by preferred directions, and hence anisotropies

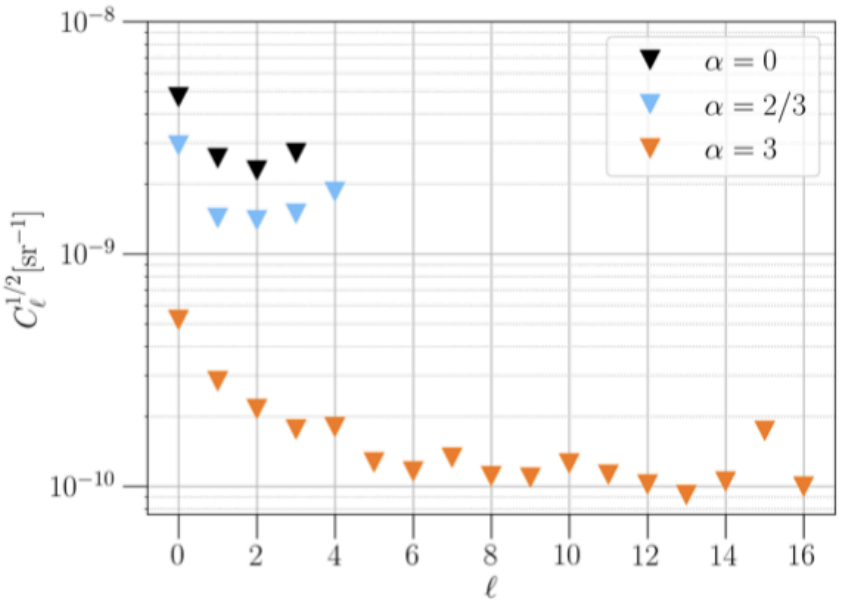

95% upper limits on C_ℓ for different α using combined O1+O2+O3 data

$$\Omega_{\mathrm{GW}}(\nu) = \Omega_{\mathrm{ref}} \left(\frac{\nu}{\nu_{\mathrm{ref}}} \right)^{\alpha}$$

Diffraction-limited angular resolution Θ on the sky:

$$\theta = \frac{c}{2Df} \qquad \ell_{\max} = \frac{\pi}{\theta}$$

distance between detectors

most sensitive frequency

LVC PRD 104 (2021), 2, 022005

Mairi Sakellariadou

Anisotropies in the GW Background: info about large-scale-structure

Gravitational wave sources with an anisotropic spatial distribution lead to a GWB characterised by preferred directions, and hence anisotropies

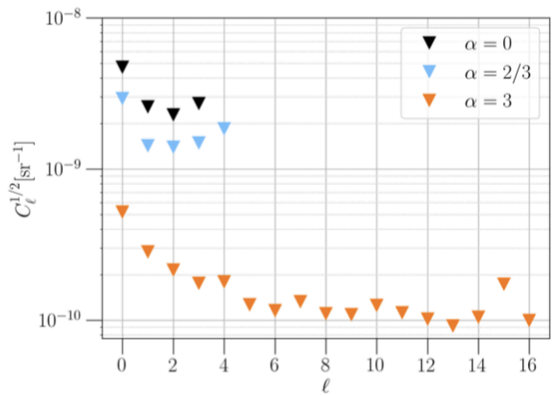

$$\boxed{\alpha = 2/3,}$$

$$\boxed{C_\ell^{1/2} < 1.9\times10^{-9}\,\mathrm{sr}^{-1},}$$

LVC PRD 104 (2021), 2, 022005

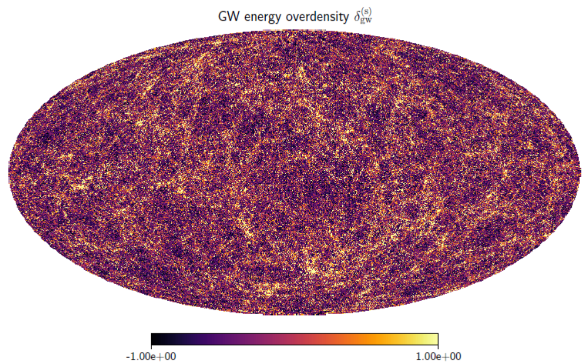

Angular resolution: 13.7 arcminutes ---- 7.3 galaxies per pixel

But theoretical studies:

$$\boxed{C_\ell^{1/2} \sim 10^{-12}\,\mathrm{sr}^{-1} \;\; \text{for } 1 \leq \ell \leq 4,}$$

if the normalised GW energy density due to an isotropic GWB of CBC is $\sim 10^{-9}$

Jenkins, Regimbau, Sakellariadou, Slezak, PRD 98, 063501 (2018)

Anisotropies in the GW Background

Gravitational wave sources with an anisotropic spatial distribution lead to a GWB characterised by preferred directions, and hence anisotropies

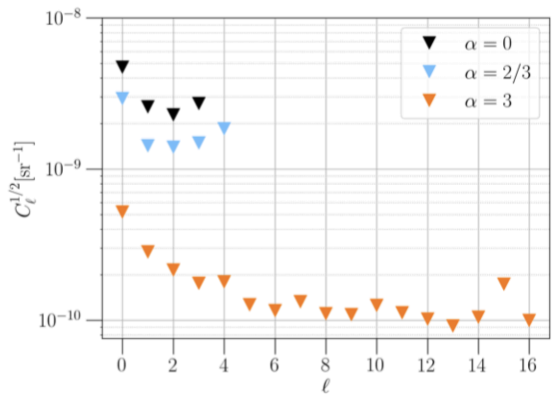

Anisotropies largely independent of the cosmic string loop distribution model

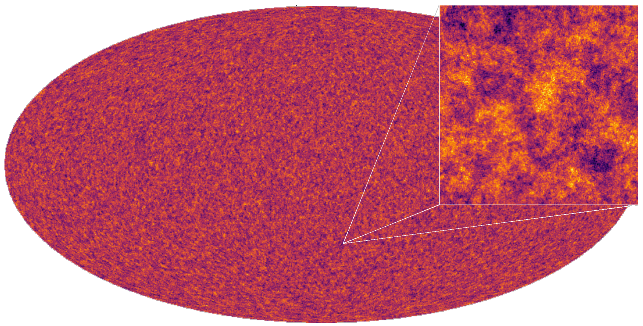

$\alpha = 0$

$$C_1^{1/2} < 2.6 \times 10^{-9}\,\mathrm{sr}^{-1}$$

LVC PRD 104 (2021), 2, 022005

But theoretical studies:

$$C_1^{1/2} \lesssim 10^{-12}\mathrm{sr}^{-1}$$

using that the isotropic component of SGWB imposes $G\mu \lesssim 4 \times 10^{-15}$

The dipole is kinematically caused by the peculiar motion of the Earth

Jenkins, Sakellariadou, PRD 98, 063509 (2018)

Conclusions

A detection of the GWB from unresolved compact binary coalescences is expected to be made by Advanced LIGO and Advanced Virgo at their design sensitivities

- **Detecting a GWB in the presence of correlated magnetic noise**

- **Simultaneous estimation of astrophysical and cosmological GW backgrounds with terrestrial interferometers**

- **GWB will give information about astrophysical models (compact binaries), beyond the standard model particle physics (cosmic strings, phase transitions), large-scale-structure, early universe cosmology (inflation, parity violation), gravity theories**

- **Isotropic and directional searches are an ongoing effort of the LIGO/Virgo/KAGRA Collaboration**